NUCLEAR SCATTERING RADIOGRAPHY

D. Garreta
DPHN/ME - CEN Saclay

INTRODUCTION

Nuclear Scattering Radiography (NSR) consists in producing three dimensional radiographies of samples that can be large by using medium energy protons beams (Ep of the order of 1 GeV) and standard particle physics detection systems.

After the first work done at CERN (Geneva)[1,2] and SIN (Zurich)[3] this techniques has been applied at Saclay to anatomical specimen [4,5] and heavy materials [5,6]. For medical applications low radiation dose and fast data acquisition are required. A first step in this direction was done at CERN [7,8] where the solid angle of the detection was increased so that the radiography of a human head could be obtained with a radiation dose of 0.3 rad, which is satisfactory, and a faster acquisition rate but still leading to a prohibitive exposure time. Further improvement, in preparation at Saclay by the same experimental team, aims, by increasing the acquisition rate, to obtain such a radiography in 20 minutes which would allow *in vivo* applications.

PRINCIPLE OF THE METHOD (see Fig. 1)

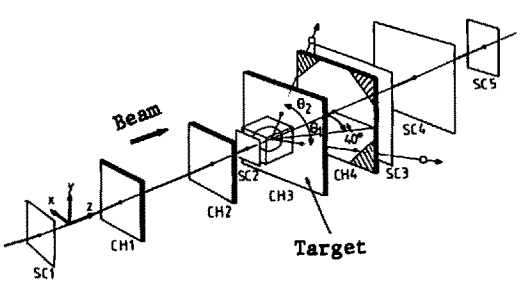

Fig. 1 : Schematic drawing of the experimental set-up of Ref 7-8, showing the set of scintillators (SC1 to 5) that trigger the position sensitive multiwire proportional chambers (CH1 to 4) used to detect the incident and scattered protons.

The principle of the method consists in illuminating the sample of which one wants to have a picture with a beam of medium energy proton. Most of them will go across the sample with just a small angular deviation due to multiple coulomb scattering but some of them will experience nuclear scattering and will go out with a direction quite different from the incoming one. So if one detects proton trajectory before the sample (in counters CH1 and CH2) and after the sample (in counters CH3 and CH4) one can get the coordinates X, Y and Z of the point where the nuclear scattering took place. Therefore it is possible

to count these events and store them in a three dimensional matrix n (X,Y,Z) corresponding to the countings from cells of dimensions ΔX, ΔY, ΔZ centred on the point of coordinates X, Y, Z. After corrections of possible inhomogeneity in the beam density distribution, absorptions of the incoming and outgoing protons in the sample and variation of the detection efficiency across the sample, this matrix is a direct measurement of the three dimensional *nuclear scattering density* distribution D (X,Y,Z) of the sample. The definition of D(X,Y,Z) is :

$$D(X,Y,Z) = \sum_i \frac{d_i\ (X,Y,Z)}{A_i}\ \sigma_R^i$$

where d_i (X,Y,Z) is the partial density of element with atomic mass A_i, σ_R^i is the nuclear reaction cross section for giving a charged particle in the detection system.

In addition to this information it is possible to get the hydrogen density distribution in the sample. When the nuclear scattering takes place on a free proton (from a hydrogen atom) the scattered and recoil protons are coplanar with the incident one and their angles θ_1 and θ_2 are related by : $tg\theta_1 \cdot tg\theta_2 = 1/\gamma^2$ (where γ is the relativistic factor in the transformation from the CM to Lab systems). These two conditions do not hold when the two protons come from quasi-free scattering on a proton bound in a nucleus because of the Fermi momentum. Therefore the subset of events which fulfill these conditions will give a measurement of the hydrogen density distribution in the sample.

Looking at the accuracy with which the coordinates of the point where the nuclear scattering took place are determined, the resolution in the transverse direction (XY plane) is determined by the resolution of the position sensitive counters CH1 to CH4 and the multiple scattering in the sample, the resolution in the beam direction Z is equal to the transverse resolution divided by $\sin\theta$. Therefore small angle scattering has to be rejected in order to keep a reasonable resolution in the Z direction. This limits the energy of the incident protons because the higher the energy the faster is the decrease of the cross section with angle.

An interesting figure is the ratio between the number of detected events n and the incoming protons N on a sample of thickness t and density d :

$$\frac{n}{N} = 6.10^{23}\ t \cdot \frac{d}{A} \cdot \sigma_R$$

It is of the order of 1 % for t = 1 cm for organic compounds for which σ_R/A is about $1.5\ 10^{-26}$ cm^2 with 650 MeV protons detected in an angular range of 15^0 to 40^0 [1] and drops down to about 0.5 % at 1 GeV but is so that the number of *usefull* protons is still relatively high (about 10 % for a human head at 1 GeV).

One must also keep in mind that for medical applications, the variations in nuclear scattering density that will be looked for are of the order of a few percent so that most of the problems will come from statistics, directly related to radiation

dose and time of exposure.

ADVANTAGES AND LIMITATION OF THIS METHOD

- One of the greatest advantages of this method clearly appears on Fig. 2 which shows absorption coefficients of different probes as a function of the atomic mass of the sample.

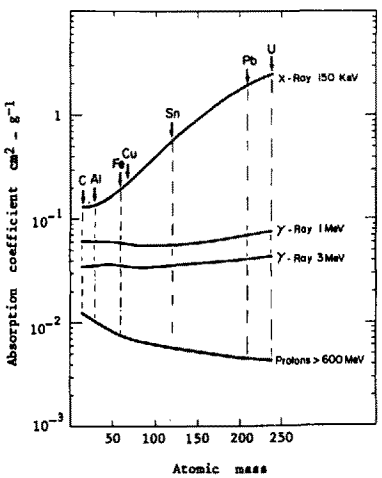

Fig. 2 : Absorption of different probes through material as a function of the atomic number A of the material.

In the case of heavy elements, the transmission coefficient of 3 MeV-γ-rays through a 10 cm copper block is only 4 % when it is still more than 50 % for the protons. For a 5 cm thick Uranium block this transmission coefficient will be less than 2 % for the γ-rays and still 2/3 for the protons.

This low absorption, very useful in the case of heavy elements, is also interesting in the case of medical applications where it makes absorption corrections rather low. For instance absorption of X-rays in the bones is so large that it can produce artefacts in Computer Assisted Tomographies (CAT) of the head, making difficult the detection of tumors located near the skull, when overall corrections in the NSR of a human head were smaller than 20 % [7].

- An other advantage of this method is the true three dimensional character of the information which allows the display of the image along any direction by simple data handling. The only anisotropy in the data is the spatial resolution which is larger along the beam direction, but there is none of the artefacts that can be generated when building a three dimensional image from independent two-dimensional cross-sections.

- The hydrogen density measurement is also an advantage but the small counting rate of such events is a serious limitation. From this point of view NMR imaging might be in much better shape although the two informations are not identical since the hydrogen density produced by NMR depends on the chemical constituents to which the hydrogen atoms belong when there is no such dependence in NSR, therefore comparison between the two informations might be interesting.

- The possibility of focussing the beam only on the useful part of the sample so that only this part and its shadow through the rest of the sample is irradiated is also interesting. In CAT for instance, a full cross section of sample has to be

irradiated. Radiography of the Spine is a case where this possibility would be very useful.

- A strong limitation in the use of NSR is obviously the need of a medium energy proton beam. On existing high energy accelerators there is no problem to get such beams because they are of low intensity and do not require any special qualities so that parasite beams can be used which do not disturb the other users of the accelerator. But there are only few available in the world.

- Another limitation is the data acquisition rate. Data of Ref 4, 5, 6 were recorded at a rate of about 100 events/sec, those of Ref 7, 8 at a rate of 1 500 events/sec, the limitation comes from the on line computing time necessary to get the coordinates of the interaction vertex (350 μs to 1 ms, depending on the complexity of the event). In the next step this time should be reduced to less than 10 μs which should allow a rate of 10^5 events/sec (producing a radiography of 10^8 events, about the number of events necessary for a human head, in 20 minutes). This is not bad when one realizes that the total volume in the latter case is about 5 l and about 50 conventional CAT would be necessary to scan the same volume. Using the possibility of focussing the beam one can restrict this volume and the recording time will be decreased in the same proportion since it is the total rate of acquisition which is limited. By using a fast specialized hardware processor it might also be possible to reduce again this time by a factor of ten, but the problem will then come from the chambers which will have to stand a beam of 10^7 p/sec.

- Multiple Coulomb Scattering (MCS) is also a limitation because it spoils the spatial resolution. It is not severe in the case of medical applications because the spread in transverse position (XY plane) induced by MCS in 10 cm of water is only 0.5 mm (fwhm) for 1 GeV protons and goes up to 1.6 mm for 300 MeV protons. For heavy material it becomes more serious, 2.4 mm and 5 mm for 10 cm of copper and uranium with 1 GeV protons. This effect which goes like the power 3/2 of the thickness, can be reduced by calculating the distance between the incoming and outgoing tracks and rejecting the events for which this distance is too large, but more beam exposure will be necessary to get the same statistics. It is also possible to restore the resolution by using deconvolution techniques.

EXPERIMENTAL SET-UP AND DATA ANALYSIS

Fig. 1 is a schematic drawing of the experimental set-up used in Ref 7, 8. A set of fast counters (scintillators SC1 to SC5 in coincidence or anticoincidence with a resolution time of the order of a few nsec) detects the incident protons which have scattered with a minimum angle of about 15^0. The coincidence signal from the scintillators triggers the four multiwire proportional chambers CH1 to 4 which give the horizontal and vertical positions of the tracks with an accuracy of 1.27 mm for the

incoming proton and 2 mm for the outgoing particles (these correspond to the wire spacing of the MWPC). The maximum volume that can be radiographed is determined by the size of chambers CH1 and CH2 (20 x 20 cm^2) and the room remaining free between chambers CH2 and CH3 (of the order of 40 cm). Then the coordinates X, Y, Z of the reaction point are calculated as well as the conditions which determine wether or not this scattering occured on hydrogen and the corresponding cell of the proper matrix is incremented. Along with these three dimensional matrices n (X,Y,Z) and n_H (X,Y,Z), the beam profile at the centre of the sample determined with CH1 and CH2 is recorded in a two dimensional matrix b (X,Y). The fact that the beam divergence is small is used to assume that the beam profile is independent of Z on the dimension of the sample. If it were not so, it would be necessary to record the profile in a set of XY planes at different Z positions and use interpolation for beam correction.

Then, a set of corrections is applied to the matrices :

- Beam correction : the matrix has to be corrected for beam intensity inhomogenity.

- Corrections for particle absorption, solid angle and mean scattering angle variation across the sample : since the absorption is rather low and not strongly dependent on the material, the overall correction for all these effects is assumed to be a smooth function of X, Y, Z and is determined empirically.

It is done by fitting a correction function f (X,Y,Z), chosen with such an analytical form that it can only reproduce smooth variations and not the local fluctuations of the type we are looking for, to the countings of either a *phantom* target which has approximately the shape and mean density of the sample or directly on some parts of the sample itself of which we know that they should have in average a constant density. When looking for defects in heavy material pieces which otherwise are homogeneous the latter solution is straight forward, for medical applications it is a bit more delicate and might depend on the specific case. In Ref 7, 8 where the sample was a human head, it was assumed that the mean density of soft tissues was constant over the whole sample, cells containing soft tissue were selected and used for the fit of the correction function (which was of second order in X, Y, and Z). The maximum correction was 20 % and the spread in the density distribution of soft tissues which was 30 % in the raw data was reduced to 13 % after correction (statistical fluctuation are of the order of 11 %).

- Corrections for statistical fluctuations and resolution improvement. The simplest way of decreasing statistical fluctuations is smoothing. To see the effect, we can look at a one dimentional smoothing of the type :

$$S_n = \tfrac{1}{4} O_{n+1} + \tfrac{1}{2} O_n + \tfrac{1}{4} O_{n-1}$$

(S_n and O_n correspond to channel n of the smoothed and original arrays respectively). The statistical fluctuations on S and O are related by $\sigma_s^2 = 3/8\ \sigma_o^2$. This means that the countings of O should be increased by a factor of 8/3 to decrease the relative statistical fluctuation to the level of S. But if we look at the fluctuations on the *difference* between two adjacent channels $\Delta O = O_{n+1} - O_n$ *which is a very important*

quantity for imaging we see that $\sigma_{\Delta o}^2 = 2\sigma_o^2$ but $\sigma_{\Delta s}^2 = \frac{1}{4}\sigma_o^2$, therefore $\sigma_{\Delta s}^2 = 1/8\sigma_{\Delta o}^2$ which means that in order to reduce the fluctuations on the difference between two adjacent channels to the level of S the counting rate on O should be increased by a factor of 8. The trouble with smoothing is the loss in resolution.

A different way of reducing statistical fluctuation and improving at the same time the resolution is to Fourier transform the spatial density distribution and apply a filter to the frequency density distribution. This filter will have the shape of the inverse of the Fourier transform of the experimental spatial resolution in the low frequency domain in order to restore some of the spatial resolution lost in the experiment, and will cut the high frequency part of the distribution to decrease the high frequency statistical fluctuations. An alternative way of restoring spatial resolution is to reproduce the experimental density distribution by the convolution of the known experimental spatial resolution with the *true original* density distribution that is looked for. These techniques are delicate and have to be used with great care because they can easily generate artefacts.

EXPERIMENTAL RESULTS

1 - Heavy materials (Ref 4, 5)

Targets of very simple geometry were used to test the effect of MCS on spatial resolution and the capability of this method to detect defects in heavy materials.

Copper blocks shown on Fig. 3 were used to test the ability of detecting narrow defects. Fig. 4 shows the density distribution along Z axis. Fig. 4a is the raw data, on Fig, 4b where the data is corrected for particle absorption and smoothed one can easily see that the depth in the density is proportional to the width of the defect which is expected when this width is much smaller than the resolution. A preliminary test of deconvolution of the density distributions by the longitudinal resolution function is shown on Fig. 4c. From these density distribution the positions of the defects can be measured with an accuracy better than 1 mm.

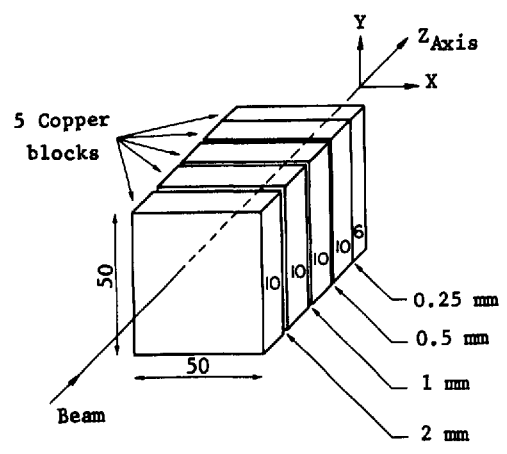

Fig. 3 : Geometry of the copper target which consists of five blocks with 50x50mm^2 cross section. Four blocks have a thickness 10 mm, the last one 6 mm. The blocks are parallel to the XY plane and separates successively by 2, 1, 0.5, 0.25 mm air intervals.

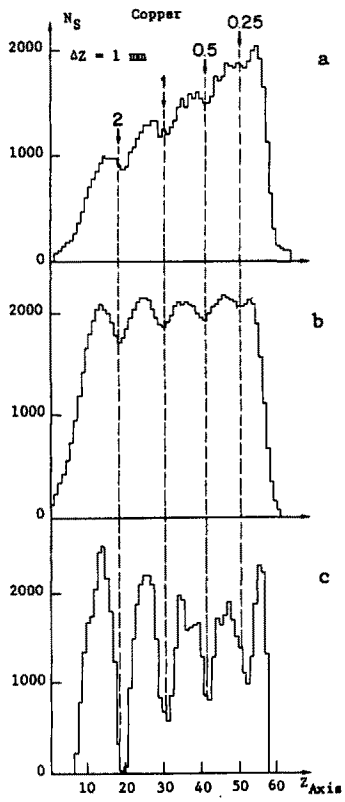

Fig. 4 : Detection and longitudinal localisation of defaults in copper.
-4a- gives the brute counting rate N_S in function of Z. On
-4b- N_S has been corrected for particle absorption ans smoothed twice to decrease statistical errors. Default thickness are indicated in mm. Channel width ΔZ=1mm. The four defaults are clearly detected and precisely located.
-4c- Deconvolution of the N_S (Z) spectrum of copper target shown on Fig. 4b by a gaussian function with FWHM about 6 mm corresponding to the experimental longitudinal resolution.

2 - Radiography of a human head (Ref 7,8)

The experimental set up was that described above (Fig. 1). The solid angle of the detection system was about 1.1 steradian corresponding to scattering angle ranging from 15^0 to 40^0. This large solid angle was chosen to minimize the radiation dose. The anatomical specimen, surrounded by low density expanded polystirene (.03 g/cm^3), was placed in a plexiglas box filled with formalin. Therefore the quantity of material surrounding the sample was very low so as to be as close as possible of *in vivo* radiography conditions.

A three dimensional radiography of a human head has been taken. The total number of events is 1.3 10^8, which corresponds to about 20 events/mm^3, they are stored in a matrix made of 124 x 124 x 96 = 1.48 10^6 cells of dimensions 1.4 x 1.4 x 2.8 mm^3 = 5.5 mm^3. About 6.5 10^6 events corresponding to scattering from hydrogen are stored in a matrix made of cells twice as large (with a volume of 44 mm^3). The radiation dose delivered during this radiography was 0.3 rad. This low radiation dose is due to the fact that 1 GeV protons are close to minimum ionisation, the cross section of the main reaction used for radiography (quasi-free scattering) is large, the information is very direct and total absorption is small. For X-rays, the information is integrated over the whole thickness of the sample and, due to strong absorption, it is necessary to deliver high radiation dose at the input of the sample in order to get a reasonable intensity at the output.

Fig. 5b and 5d represent XY cross sections, 5.6 mm thick, corresponding to the CAT presented on Fig. 5a and 5c taken from the same anatomical specimen. The hypodensisties that can be seen at the centre of left and right lobes of the brain on Fig. 5c, also show up clearly on Fig. 5d. On the other hand statistically significant density variations show up on the soft tissues of Fig. 5,

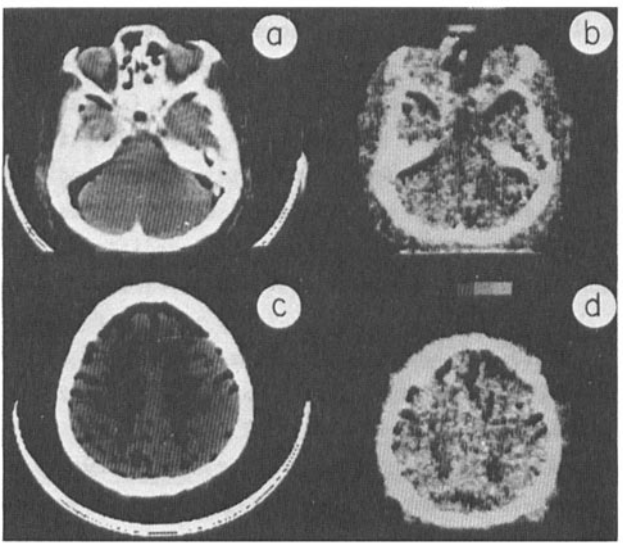

Fig. 5 : Fig. b and d : XY (horizontal) slices of the head obtained by NSR. Slice thickness is 5.6 mm and pixels are 1.4 x 1.4 mm^2. Each grey tone corresponds to a nuclear density variation of 4 %. Fig. a and c : XY slices of the same head approximately at the same level obtained by X-ray scanner.

one level of brightness represents a variation of 4% in the density for the NSR. On Fig. 6 and 7 one level represents 4 %. Fig. 6 represents a ZX cross section (Fig. 6a), 2.8 mm thick, on which the beginning of the spine is clearly seen, and a ZY cross section (Fig. 6b) of the same thickness on which one can see the chin. These views show the capability given by NSR to provide directly cross sections along any direction. Fig. 7b and 7d represent XY cross sections for the hydrogen density, Fig. 7a and 7c are the corresponding cross sections for the normal events. On the hydrogen density pictures, bones appear dark, as expected, but one can also notice statistically significant structures with hypodensities different from the ones observed on the normal events.

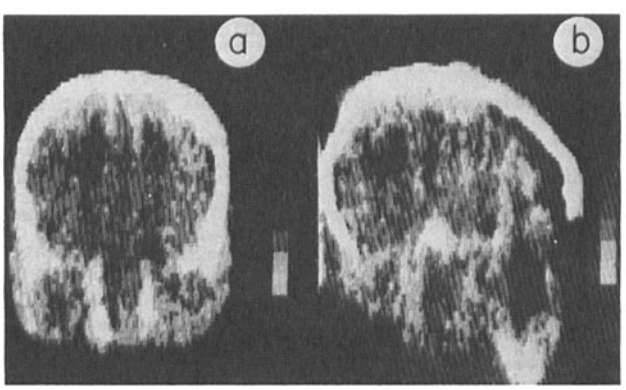

Fig. 6 : a- XZ(frontal) slice of the head obtained by NSR. b- ZY(sagittal) slice. Thickness is 5.6 mm and pixels are 2.8 x 1.4 mm^2. Each grey tone corresponds to a nuclear density variation of 4 %.

CONCLUSION

NSR techniques has reached a point where it seems to have interesting applications in metallurgy. For medical applications, improvement of the data acquisition rate should make it useful for specific cases where the screening of bones makes X-rays radiography difficult, for instance for spinal cord or tumours

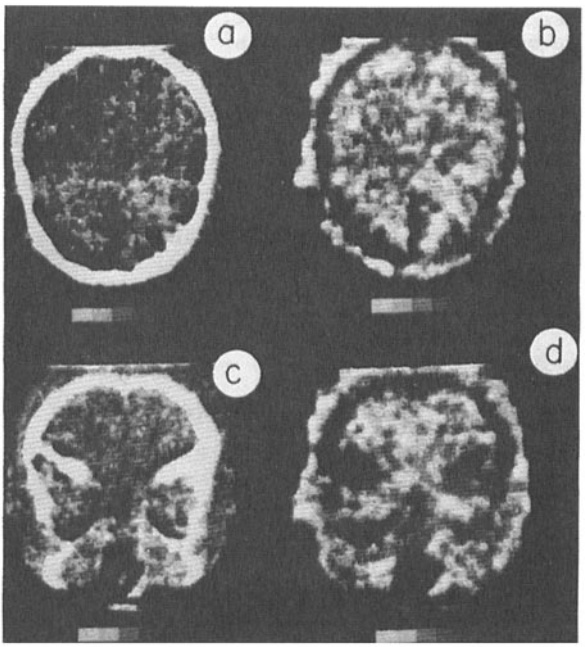

located near the skull. But the quality of *nuclear scattering density* information has to be tested on a large number of samples.

Fig. 7 : XY slices at two different levels. Thickness is 11.2 mm and pixels are 1.4 x 1.4 mm^2. Each grey tone corresponds to a counting variation of 4 %.
a - c - simple radiographs, b - d - hydrogen radiographs. Geometry of b and d are respectively identical to the one of a and c. On b and d bone appears black because it has a small water content and so for hydrogen.

REFERENCES

1 - J. Saudinos, G. Charpak, F. Sauli, D. Towsend, J. Vinciarelli. Nuclear scattering applied to radiography. Phys. Med. Biol. 20 : 890-905, 1975.

2 - G. Charpak, S. Majewski, Y. Perrin, J. Saudinos, F. Sauli, D. Towsend, J. Vinciarelli. Furhter results in nuclear scattering radiography. Phys. Med. Biol. 21 : 941-948, 1976.

3 - L. Dubal. Protoscopie : Annual report, Schweizerisches Institut für Nuklear-forschung (S.I.N.), Villigen, Switzerland, B 14-16, 1976.

4 - J. Berger, J.C. Duchazeaubeneix, J.C. Faivre, D. Garreta, D. Legrand, M. Rouger, J. Saudinos, C. Raybaud, G. Salamon. Nuclear scattering radiography of the spine and sphenoid bone. Journal of computer assisted tomography : 2 488-498, September 1978.

5 - J. Berger, J.C. Duchazeaubeneix, J.C. Faivre, D. Garreta, D. Legrand, C. Raybaud, M. Rouger, G. Salamon, J. Saudinos. Radiographie par diffusion nucleaire. Compte rendu d'activité du département de Physique nucléaire. 1976-1977, note CEA-N-2026 p 263.

6 - J.C. Duchazeaubeneix, J.C. Faivre, D. Garreta, B. Guillerminet, D. Legrand, M. Rouger, J. Saudinos, J. Berger. Submitted for publication in "Materials evaluation".

7 - G. Charpak, J.C. Duchazeaubeneix, J.C. Faivre, D. Garreta, B. Guillerminet, G. Odyneic, P. Palmieri, Y. Perrin, C. Raybaud, M. Rouger, G. Salamon, J.C. Santiard, J. Saudinos, F. Sauli. Radiographie par diffusion nucleaire. Compte rendu d'activité du département de Physique nucléaire. CEA Saclay, to be published.

8 - F. Sauli. Progress in nuclear scattering radiography. International Conference on Computing tomography. Pavia. Oct. 9.10.1978.